City Research Online

City, University of London Institutional Repository

Citation: Sa'ad, M. S. M., Ahmad, H., Samion, M. Z., Alias, M. A., Zaini, M. K. A., Sing, L. K., Grattan, K. T. V., Rahman, B. M., Brambilla, G., Harun, S. W. & et al (2023). A fiber Bragg grating-based inclinometer probe with enhanced sensitivity for a higher slope profiling resolution. Sensors and Actuators A: Physical, 364, 114804. doi: 10.1016/j.sna.2023.114804

This is the accepted version of the paper.

This version of the publication may differ from the final published version.

Permanent repository link: https://openaccess.city.ac.uk/id/eprint/31721/

Link to published version: https://doi.org/10.1016/j.sna.2023.114804

Copyright: City Research Online aims to make research outputs of City, University of London available to a wider audience. Copyright and Moral Rights remain with the author(s) and/or copyright holders. URLs from City Research Online may be freely distributed and linked to.

Reuse: Copies of full items can be used for personal research or study, educational, or not-for-profit purposes without prior permission or charge. Provided that the authors, title and full bibliographic details are credited, a hyperlink and/or URL is given for the original metadata page and the content is not changed in any way.

City Research Online: http://openaccess.city.ac.uk/ publications@city.ac.uk

A fiber Bragg grating-based inclinometer probe with enhanced sensitivity for a higher slope profiling resolution

Muhammad Syamil Mohd Sa'ad[a], Harith Ahmad[a,*], Muhamad Zharif Samion[a], Mohamad Ashraff Alias[a], Muhammad Khairol Annuar Zaini[a], Lim Kok Sing[a], Kenneth T.V. Grattan[b], B.M. Azizur Rahman[b], Gilberto Brambilla[c], Sulaiman Wadi Harun[d], and Mohammad Faizal Ismail[a]

[a]*Photonics Research Center, Universiti Malaya, 50603 Kuala Lumpur Malaysia*
[b]*School of Mathematics, Computer Science & Engineering, City, University of London, London, EC1V 0HB United Kingdom*
[c]*Optoelectronics Research Center, University of Southampton, Southampton SO17 1BJ, United Kingdom*
[d]*Department of Electrical Engineering, Faculty of Engineering, Universiti Malaya, 50603 Kuala Lumpur Malaysia*

**Corresponding Author: harith@um.edu.my*

Journal Pre-proof

Abstract

A fiber Bragg grating (FBG)-based inclinometer probe with enhanced sensitivity has been developed for slope or ground movement monitoring. The inclinometer probe utilized six FBGs for the tilt measurement and a strain-free FBG that provided the temperature compensation factor. The inclinometer probe was fabricated entirely using a 3D printer and can fit into the standard inclinometer casing, which can be placed into the boreholes. The dimension of the probe is similar to the conventional inclinometer probe, with a total length of 70 cm. Additionally, this design was equipped with three highly compact tilt sensors within the same probe length, providing a better resolution of the inclination profile. Each tilt sensor possesses a flexible middle shaft fabricated using thermoplastic polyurethane (TPU) and was equipped with two FBGs for bi-directional tilt angle measurement (+x and -x). Initially, the tilt sensor was calibrated in the laboratory, which yielded a sensitivity value of 0.0215 nm/°. This value is higher than most previous designs by a factor of two because of the middle shaft's elasticity, which can induce a more significant strain on the FBG. The horizontal displacement of a conventional inclinometer casing could be observed during the field test, which proves the device's functionality. The results have indicated that the inclinometer can be applied in several geotechnical applications, particularly ground movement monitoring.

Keywords: Fiber Bragg grating, inclinometer, tilt sensor, 3D-print, Polylactic Acid, Thermoplastic Polyurethane.

1. Introduction

In structural health monitoring, inclinometers are widely used to measure and monitor the inclination angle of slopes, building structures, and construction sites [1]. Inclinometers are typically categorized into two types: the probe and in-place inclinometers. They are utilized to obtain a slope profile, the 2D representation of the slope [2,3]. In conventional probe inclinometers, the probe, typically 70 cm long, is usually equipped with a single MEMS sensor. They are also fitted with spring-pressured wheels to descend along a pre-installed inclinometer casing buried in a borehole [4]. At certain depth intervals, measurements are taken between two depth points to determine the inclination angle. This procedure is typically done manually on-site.

On the contrary, in-place inclinometers are installed permanently where ground movements are expected to occur. Owing to the recent technological advancement, measurements can be taken remotely and continuously, eliminating unnecessary risks at the sites [5]. A conventional, electrical-based inclinometer can determine the inclination angles by measuring the sensor's magnetic effect [6]. However, significant voltages or high electromagnetic interference from adjacent power lines could compromise the performance and accuracy of these sensors [7]. It limits their applications in ground movement monitoring.

Recently, optical fiber-based sensors have become a preferred alternative to traditional mechanical and electrical sensors in ground movement applications since they are insensitive to electromagnetic interference. Numerous optical fiber-based sensors have been proposed in civil and structural health engineering. These include Brillouin's scatter-based distributed sensors [8,9], Michelson interferometer sensors [10], Fabry-Perot strain sensors [11], and Fiber Bragg Grating (FBG) sensors [12–21]. FBGs are considered one of the best options in sensing applications because of their multiplexing capabilities and their ability for long-distance monitoring [22]. Researchers have designed and proposed several FBG-based tilt sensors in the past. For example, S. He *et al.* [14] proposed a tilt sensor design using a 200g weight suspended from a circular top plate by three FBGs. Their sensor was calibrated over -15° to 15° in one direction. In another work, Bao *et al.* [23] used four FBGs aligned in parallel, with an equal distance between each FBG. Their sensor was tested for a tilt measurement range from -40° to 40° tilt angle towards the x-z and x-y planes. However, both designs utilized

Journal Pre-proof

a pendulum-like structure without any additional configuration that could prevent unwanted bends and twists of the FBGs. Therefore, it would lead to erroneous measurements. Besides, the sensing unit, the FBGs, are left hanging unprotected without any casings or cover that could prevent any damage to the FBG structure. Since FBGs are fragile when not protected, the sensor would not survive in the harsh conditions of the monitoring sites. Their tilt sensor's designs also comprise large and bulky parts, with the structure having a height of 22 cm and a width of more than 8 cm for a single tilt sensor. It would render their sensors impractical for field use, as the diameter of a conventional inclinometer casing used nowadays is only 7 cm.

On top of this, Ismail *et al.* [20] [21] fabricated a 3D-printed, FBG-based inclinometer with a sensitivity value of 0.01 nm per degree of tilt. Four FBGs were used for biaxial tilt angle measurements and were temperature calibrated over -25°C to 80°C. The FBGs were installed along with a Polylactic Acid (PLA)-based middle shaft that would bend due to gravitational pull when tilted to a certain degree. Although the design is considered compact and suitable for real-field application, the sensor is still lacking in terms of sensitivity value due to the physical properties of PLA, which was regarded as a hard plastic with a high Young's modulus value of 2.3 GPa. This indicates that PLA is rigid and harder to bend, causing PLA-based devices to induce lesser strain on the gratings. Therefore, increasing the sensitivity value would simultaneously increase the tilt angle resolution that the device could measure. Besides, there are no reported works regarding the slope profile and borehole resolution.

This work proposed a 3D-printed, FBG-based inclinometer to address the current limitations of FBG-based inclinometers and enhance the resolution of the inclination measurements compared to conventional probe inclinometers. The inclinometer consists of three sensors, denoted S1, S2, and S3. Each sensor was equipped with two FBGs representing +x (FBG 1) and -x direction (FBG 2), giving six FBGs used for the tilt measurement. Another FBG was spliced in series with FBG 1 and FBG 2 to provide the temperature compensation factor. The inclinometer was fabricated entirely using a 3D printer, with most parts printed using PLA material. The middle shaft of the tilt sensor was fabricated using thermoplastic polyurethane (TPU) in comparison to references [20] and [21], where their midshaft was made of PLA material. The higher flexibility and elasticity of the TPU-based middle shaft would induce a more significant strain on the FBG when the sensor is tilted compared to the PLA-based material [24,25]. A more substantial shift could be observed in the FBG reflective

Journal Pre-proof

wavelength, indicating higher sensitivity towards tilt angle. Besides that, three sensors in this device enable the FBG-based inclinometer to map the ground or slope movement with better precision and resolution than conventional probe inclinometers. In a traditional inclinometer of the probe, only a single MEMS sensor was used along with the 70 cm probe, while our design comprises three sensors within the same probe length. As a result, more data at a specific borehole's depth could be acquired, indicating a higher slope profiling resolution.

Furthermore, the proposed inclinometer design is also free from unwanted bends and twists, with a width of only 5 cm, designed to fit into the conventional inclinometer casing in boreholes. Our design successfully overcomes the unwanted bend and twists in the large and bulky designs, as in references [14] and [23]. A sensitivity value of 0.0215 nm per degree of tilt was obtained during the laboratory calibration, where the sensor was tilted from 0° to 40° towards +x and -x directions. These enhancing factors would make our proposed inclinometer suitable for geotechnical applications, mainly in the ground movement monitoring for the landslides early warning system.

Journal Pre-proof

2. Fabrication of the FBG-based inclinometer

2.1. Inclinometer Design

The schematic illustration of the proposed inclinometer is depicted in Figure 1(a), while the actual image of the inclinometer is in Figure 1(b). The inclinometer has a length of 70 cm and was fabricated entirely using the 3D printer. It consists of three sensors denoted as S1, S2, and S3. S1 was connected to S2 using a 3D-printed connector fabricated using Polymax PLA. During the PLA printing procedure, the nozzle and the printing bed temperature were set at 190°C and 45°C, respectively. S2 was similarly attached to S3. The 3D-printed connector has a spring-like mechanism in the middle, which allows the sensors to bend and follow the borehole's inclination in the ground. The connectors also form a passage between the sensor and ensure that the fiber cables are fully protected from the harsh environments at the sites.

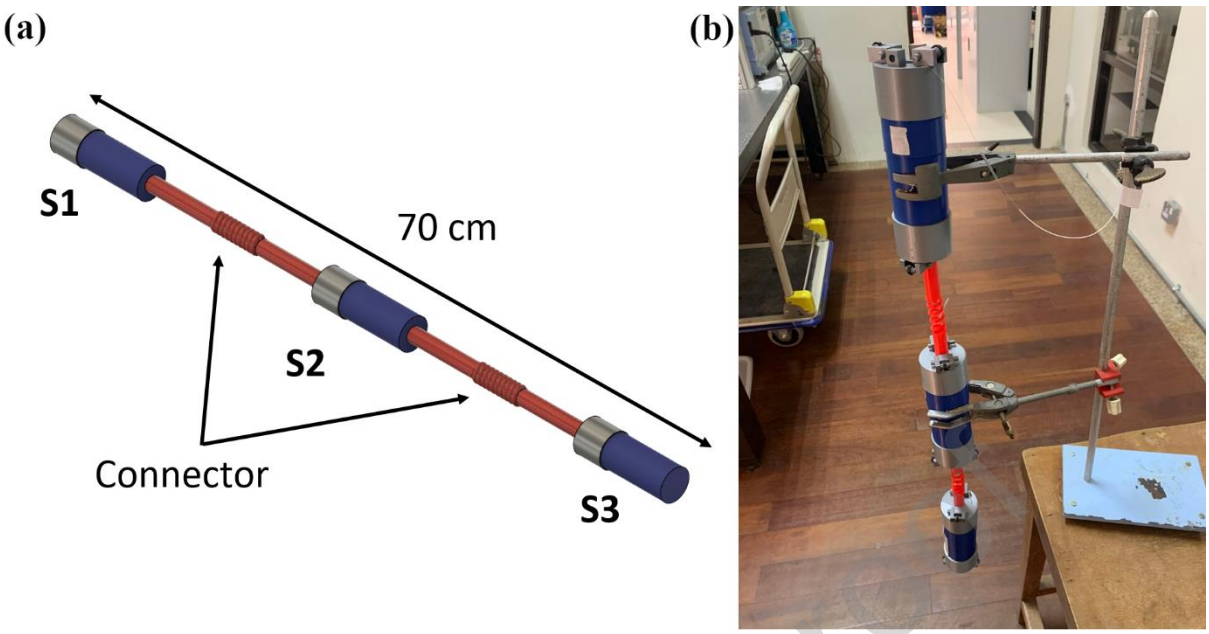

Figure 1. (a) Illustration of the proposed inclinometer with spring-like connectors, and (b) the actual picture of the inclinometer.

Journal Pre-proof

2.2. S1, S2, and S3 Design

S1 was fabricated by encapsulating a tilt sensor inside a 3D-printed cylindrical holder, as shown in Figure 2. The cylindrical holder was fabricated using a similar PLA material and consists of two parts; the top part has a length of 5 cm, while the bottom part is 13 cm. The top part is of shorter length because the tilt sensor's head needs to be attached to the top part of the holder as a fixed point, while the middle shaft and the lower part of the tilt sensor were left hanging inside the longer part of the cylindrical holder. This is to ensure that the lower part of the tilt sensor would experience a bend downwards when the sensor is tilted to a certain degree and prevent the tilt sensor from becoming twisted, which might lead to erroneous results. In addition, a longer top part would complicate the installation procedure of the tilt sensor. Therefore, the bottom part of the cylindrical holder closed the tilt sensor from the bottom, leaving the tilt sensor hanging inside the holder. S2 and S3 were fabricated using a similar approach. The final length of each device, S1, S2, and S3, is 15 cm.

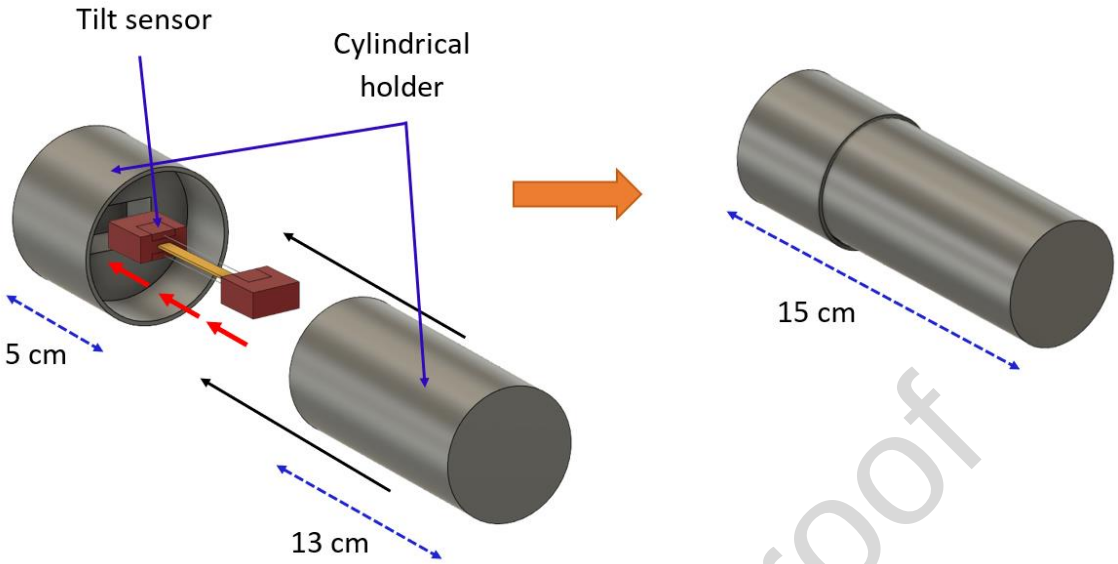

Figure 2. The installation process of the tilt sensor inside a cylindrical holder.

Journal Pre-proof

2.3. Tilt Sensor Design

The illustration of the tilt sensor design used in Figure 2 is given in Figure 3(a). The sensor was printed separately as parts A, B, C, and the sensing unit. Part A and C were designed to hold the sensing unit's end, while Part B connects Part A and C as a middle shaft. Part A and Part C were fabricated using Polymax PLA, while Part B was fabricated using PolyFlex TPU. Both were acquired from Polymaker LLC (US). In this case, during the TPU printing procedure, the nozzle and the printing bed temperature were set to 220°C and 60°C, respectively.

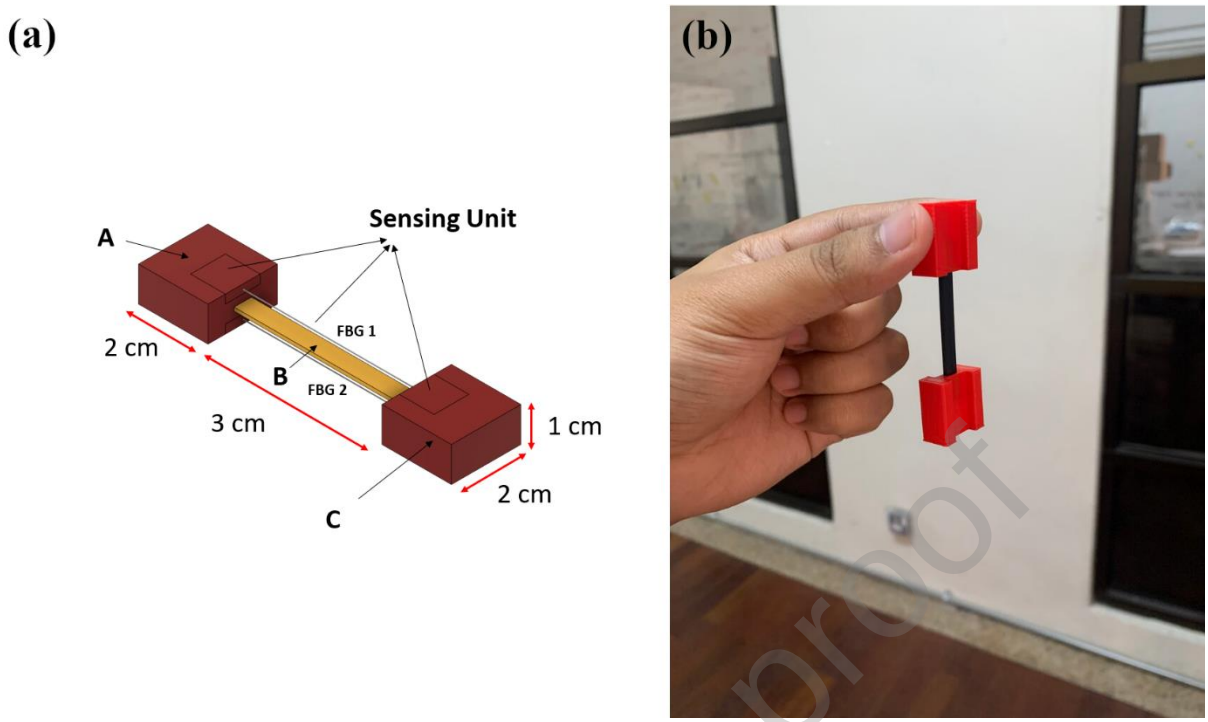

Figure 3. (a) Illustration of the fabricated sensor with a bendable, TPU-based middle shaft (part B), and (b) the actual picture of the fabricated sensor.

The sensing unit is the main sensing structure of this design, where FBGs would be installed. It was fabricated by embedding both ends of FBG 1 into the PLA in a strain-tight position. It will eliminate pre-stress errors that might arise from glue because its adhesive property tends to deteriorate over time. Figure 4 illustrates a schematic diagram of the embedding process using the 3D printer, described in detail in [26]. The fused deposition modeling (FDM) head (3D-printer printing head) feeds the filament to the nozzle using the driven wheels to extrude raw material layer by layer, as in Figure 4(a). To embed the fiber into the PLA material, the printing procedure was paused halfway so that the fiber could be laid and fixed on top of the half-printed structure, with FBG positioned at the center of the sensing unit, as illustrated in Figure 4(b). Then, the printing procedure was resumed, with both ends of the FBG fully embedded inside the PLA. During the embedding process, the reflective wavelength spectrum of the FBG used was recorded to study the FBG response. The FBGs used in this work were fabricated using the phase mask technique in which the gratings were inscribed into a hydrogenated single-mode fiber's core. A 248 nm Krypton Fluoride (KrF) excimer laser was used, whereby the laser light passed through the phase mask to create an

Journal Pre-proof

interference pattern (grating) inside the fiber's core. The gratings formed inside the core will detect any strain and temperature changes as these parameters would directly affect the spacing of the gratings, which will cause the shifting of the measured wavelength. Bragg wavelength shifts, $\Delta\lambda_B$, that associated with strain and temperature is given by:

$$\frac{\Delta\lambda_B}{\lambda_B} = K_\varepsilon \Delta\varepsilon + K_T \Delta T \tag{1}$$

where K_ε is the strain coefficient, K_T is the temperature coefficient, $\Delta\varepsilon$ is the strain change, and ΔT is the temperature change.

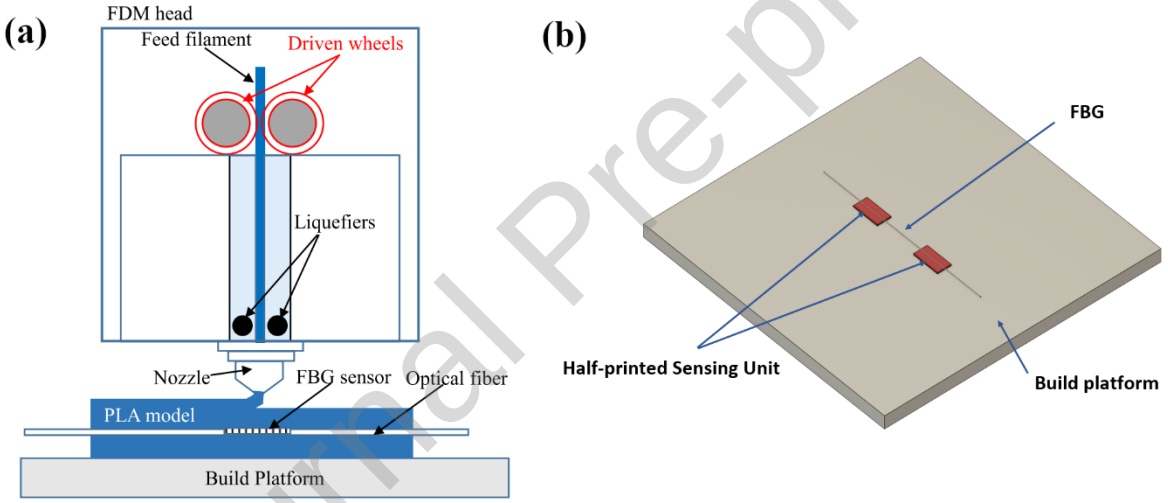

Figure 4. (a) The illustration of the FBG embedding process using a 3D printer [26] and (b) the 3D view illustration of the printing process when it was paused midway, illustrating the FBG position when it was laid on top of the half-printed PLA structure.

Journal Pre-proof

The sensing unit with an embedded FBG 1 was then installed by attaching one of its ends to Part A and the other to Part C. This procedure would cause FBG 1 to be placed along the middle shaft, parallel to Part B, as illustrated in Figure 3(a) previously. Next, another sensing unit embedded with FBG 2 was installed on the other side of the middle shaft, facing the opposite direction of FBG 1. For example, if FBG 1 faces the +x direction, FBG 2 would then face the -x direction. Figure 3(b) shows the actual picture of the fabricated tilt sensor.

3. Experimental Setup

3.1. Laboratory test and calibration

A tilt sensor illustrated in Figure 3(a) was equipped with three connected FBGs. The FBGs have a reflective wavelength of 1532.90 nm, 1538.09 nm, and 1542.46 nm and are denoted as FBG 1, FBG 2, and FBG T, respectively. FBG 1 was installed facing the +x direction, while FBG 2 was installed on the opposite side of FBG 1, facing the -x direction. FBG T was left strain-free to provide the temperature compensation factor. The sensor was attached to a digital protractor for tilt calibration. The tilt sensor was then tilted from 0° to a maximum of only 40° towards the +x direction (to the right). This is to avoid the risk of breaking the FBG. On visual inspections, when the angle was at 40°, there was an indication that the FBG may break and almost reached its tensile limit. In this context, it is essential to note that the maximum angle of the sensor depends on the material's elasticity and how much the fiber can be stretched before it breaks. A sensor with a rigid shaft based on PLA will have a more extensive range of tilt angles compared to the sensor with a less rigid shaft that is more elastic, as in the case of TPU. This is because a rigid middle shaft would cause the sensor harder to bend when tilted, inducing lesser strain onto the fiber when compared to elastic sensors. A similar concept could be applied to sensors fabricated using a more flexible material. The elastic middle shaft would pull the fiber extensively within only a short tilt angle range, causing it to reach its tensile limit earlier. This procedure was repeated with a tilt towards the -x direction (to the left). The wavelength spectra were observed using the optical spectrum analyzer (OSA).

3.2. Field test

S1 was equipped with two FBGs, denoted FBG 1 and FBG 2, having the same reflective wavelength of 1532 nm. FBG 1 represents the +x direction, while FBG 2 represents the -x direction. S2 and S3 were also equipped with two FBGs, each having the same reflective wavelength of 1538 nm and 1548 nm. FBG 1 of S1 was spliced in series with FBG 1 of S2 and joined again with FBG 1 of S3, producing one single output with three reflective peak wavelengths of 1532 nm and 1538 nm 1548 nm for the +x direction. Similarly, for the -x

Journal Pre-proof

direction, FBG 2 of S1 was connected in series with FBG 2 of S2 and FBG 2 of S3, producing one single output with three reflective wavelengths.

A conventional inclinometer casing with a length and a diameter of 6 m and 7 cm, respectively, was installed vertically onto a wall of a 3-story building. Two tests were conducted to verify the functionality of the fabricated inclinometer. Before the tests were conducted, without any horizontal displacement of the casing, the FBG-based inclinometer was inserted into the pre-installed casing from the top until a depth of 5 m, in a 0.5 m interval. During each interval, the reflective peak wavelengths of the FBGs were measured using the OSA. This measurement was considered the initial profile of the casing with a 0° inclination angle. After the initial measurement, the inclinometer was pulled back out from the case.

The first test is illustrated in Figure 5(a), where the bottom part of the casing was pulled horizontally while the top part was in a fixed position. The bottom part was pulled towards the +x direction until it reached a 0.5 m horizontal displacement from the original vertical axis. Next, the FBG-based inclinometer was inserted back into the casing until a depth of 5m in a 0.5 m interval. The casing's bending profile could be determined by analyzing the reflective peak wavelength obtained from the FBGs in the sensors. After this measurement was taken, the inclinometer was pulled out again. The bottom part of the casing was pulled again in the same direction until it reached 1 m horizontal displacement instead of 0.5 m. The inclinometer measurements were taken similarly to the 0.5 m horizontal displacement of the casing.

Journal Pre-proof

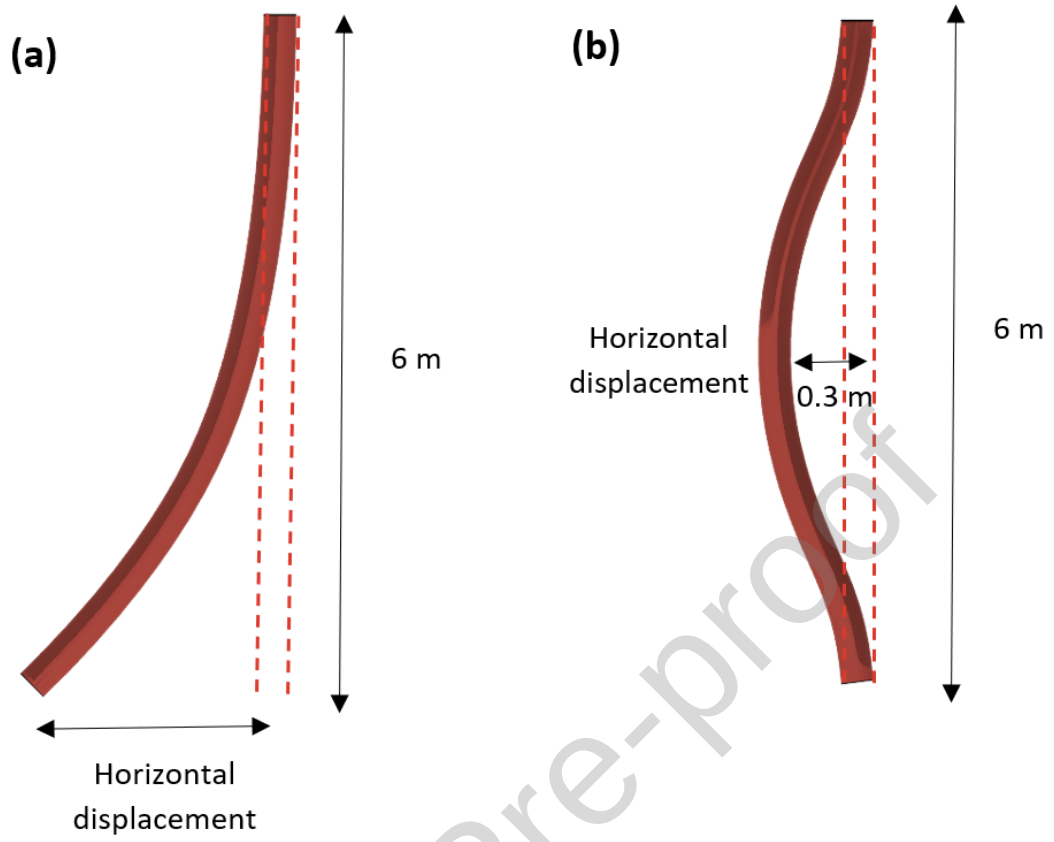

Figure 5. The illustrations of the real-field testing when (a) the casing was pulled at the bottom and (b) the casing was pulled at the middle.

Figure 5(b) illustrates the second test where the casing was pulled at the middle with fixed ends. The middle part of the casing was pulled until it reached 0.3 m in horizontal displacement. The FBG-based inclinometer was inserted 5 m into the casing in a 0.5 m interval. It is similar to Test 1, where the bending profile of the casing could be determined. However, a more significant force is needed to pull the casing more than 0.3 m as the middle part is harder to bend when both casing ends are fixed.

4. Results and Discussion

4.1. Laboratory test and calibration

Figure 6(a) shows the wavelength spectrum of FBG 1 during the embedding process before it was installed on the tilt sensor. The figure indicates that the reflective peak spectrum

Journal Pre-proof

of FBG 1 shifts during the embedding process due to the high temperature of the 3D printer's nozzle. In addition, it could also be observed that after the printing process, the reflective spectrum of FBG 1 did not return to its initial value before the embedding process occurred. It is mainly due to the shrinking of the PLA material during the cooling phase (curing). The shrinking of the PLA on both fiber ends stretches the grating in the middle, causing a slight shift in the reflective peak wavelength of FBG 1. Figure 6(b) further illustrates the shrinking process on both ends of the FBG that would eventually alter its initial value. Figure 6 verifies that FBG could withstand the embedding process into the PLA without damaging the gratings.

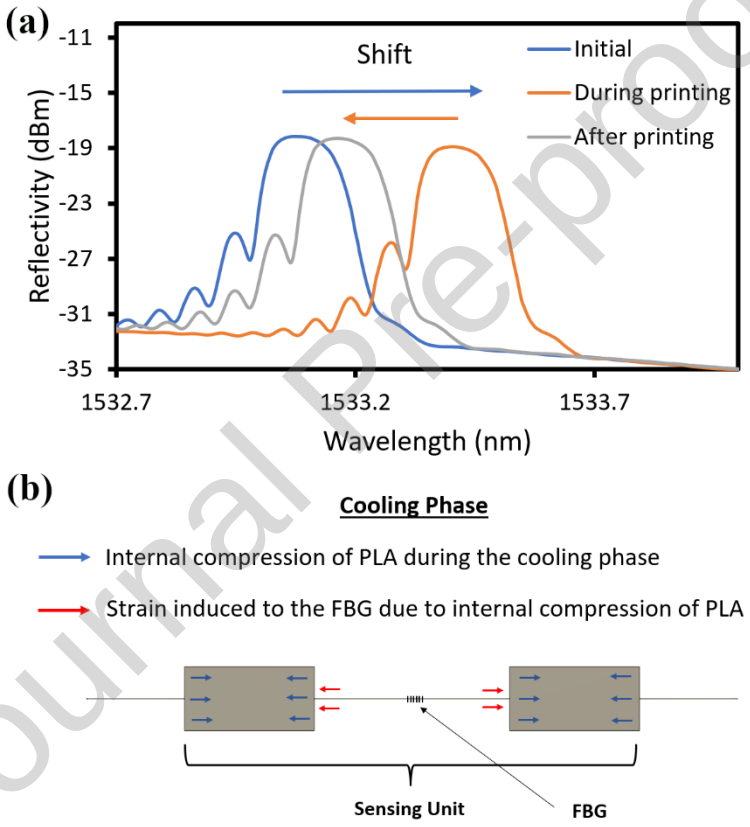

Journal Pre-proof

Figure 6. (a) The wavelength spectrum of FBG 1 during the embedding process and (b) the illustration of the strain induced on the grating during the cooling phase.

In Figure 7(a), at the initial position of 0° tilt angle, both FBG 1 and FBG 2 are subjected to initial tensional stress due to the weight of the bottom part, *W,* which is the product of the mass, *m*, and the gravitational pull, g such that $W = mg$. During tilt calibration, the top part of the sensor body is pushed towards the –x direction, as shown by the green arrow in the

diagram of Figure 7(b). Simultaneously, the bottom part of the sensor moved toward the +x direction. The initial spectrum of the sensor is given in Figure 7(c) at a tilt angle of 0°. During the tilt towards +x, the inclined position of the sensor body would cause FBG 1 to be subjected to tensile force stretching outwards, $F_{T,}$ due to the weight of the bottom part of the sensor at an angle θ. The fiber towards the +x direction would be extended due to the tensile force, F_T, and the bending moment, B acting on the middle shaft, causing an increase in the tensional stress onto FBG 1 as in Figure 7(b). This resulted in the FBG 1 reflective wavelength shifting towards the right, as shown in Figure 7(d). The zoomed-in version of the wavelength shifts depicted in Figure 8(a) indicates that FBG 1 was strained during the tilt towards the +x direction. From reference [13], the F_T and B are given by the equations below,

$$F_T = W\cos\theta, \text{ and,} \tag{2}$$

$$B = W.L\sin\theta, \tag{3}$$

where W is the weight of the bottom part, L is the bending arm length which, in this case, is the length of the middle shaft, and θ is the tilt angle. At the same time, FBG 2 will experience compression, resulting in the wavelength shift towards the left, as shown in Figure 7 (d). Furthermore, it is also evident that the strain-free FBG T did not indicate any change as it was left loose and unstrained. Therefore, it proves that FBG T would provide a temperature compensation factor for the sensor.

Journal Pre-proof

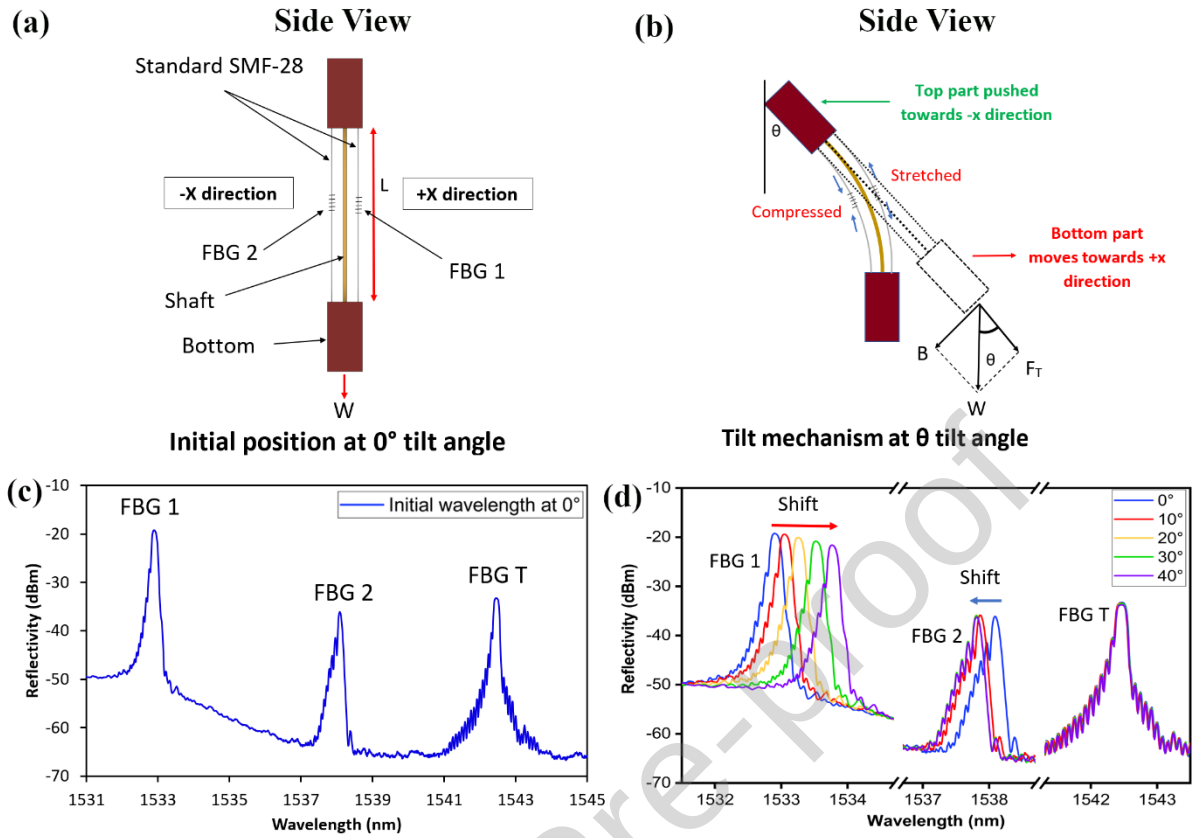

Figure 7. (a) The side view illustration of the sensor device at 0° tilt, (b) during the tilt towards +x direction, (c) the initial spectrum of the sensor illustrating FBG 1, FBG 2, and FBG T at 0° tilt, and (d) the wavelength spectrum of FBG 1, FBG 2, and FBG T when it was tilted from 0° until 40° towards +x direction.

A closer view of the wavelength shifts of FBG 1 can be observed in Figure 8(a), while a graph of wavelength shifts versus tilt angle was plotted as in Figure 8(b) to monitor the response of FBG 1 towards different tilt angles. A linear trend with a sensitivity value of 0.0215 nm/degree can be deduced from the graph, supported by an excellent R^2 value. The sensitivity value obtained is higher than PLA-based designs by a factor of two [20,21]. This is because TPU has a lower Young's modulus, making it more flexible as a middle shaft when compared to PLA [25,27]. On the other hand, a middle shaft fabricated using TPU will cause the bottom part of the sensor to exert more significant tensional stress to the FBG during the tilt and thus, increasing the sensor's sensitivity compared to a more rigid middle shaft. This has been explained by Hong et al. [13]. Since the tensile force and the bending moment cause the fiber to stretch and exert strain, ε, to the FBG, which is given by the equation below:

Journal Pre-Proof

$$\varepsilon = \frac{F_T}{EA_s} \pm \frac{B}{EI_S} \quad (4)$$

where F_T, B, E, A_s, and I_s are the tensile forces, bending moment, Young's modulus, cross-sectional area, and the moment of inertia of the sensor beam, respectively.

By referring to equation (4), dividing the tensile force and the bending moment with a smaller Young's modulus value would cause a more considerable strain and vice versa. The equation validates that a material with a smaller Young's modulus would exert a larger strain on the FBG, resulting in greater wavelength shifts and, in turn, sensitivity. On top of that, the calibration data in Figure 8(b) also validates that the sensitivity value obtained (0.0215 nm/degree) is indeed higher than the PLA-based design by a factor of two.

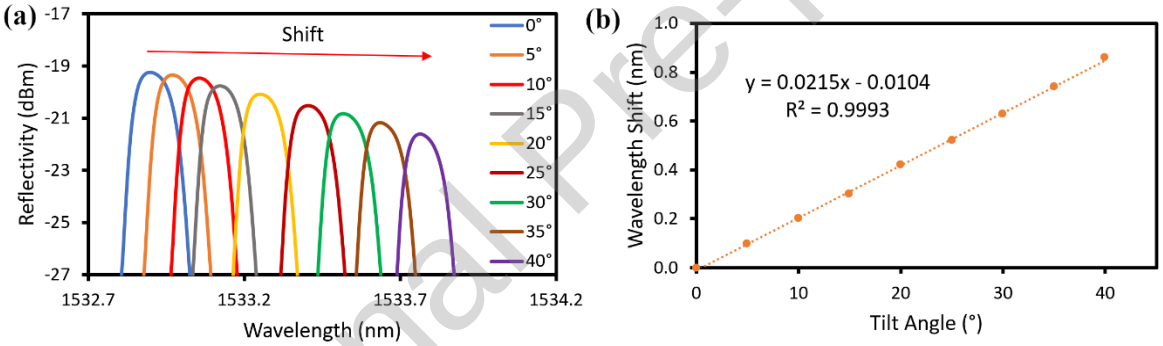

Figure 8. (a) A closer view of FBG 1 redshift during 0° to 40° tilt and (b) the linear response of FBG 1 in terms of wavelength shifts during 0° to 40° tilt.

Further, a closer view of the wavelength shift of FBG 2 in Figure 7(d) is given in Figure 9(a). From the figure, the blueshifts of FBG 2 are up until 10° of tilt, while the spectrum shows a shift close to zero for the rest of the tilt angle. Finally, the linear response of FBG 2 was plotted in Figure 9(b), where the figure shows that for a tilt until 10°, the sensor still exhibits a linear response with a perfect R^2 value. It indicates that beyond 10° of tilt towards the +x direction, the compressional force exerted onto FBG 2 exceeded the compression limit of the grating.

Journal Pre-proof

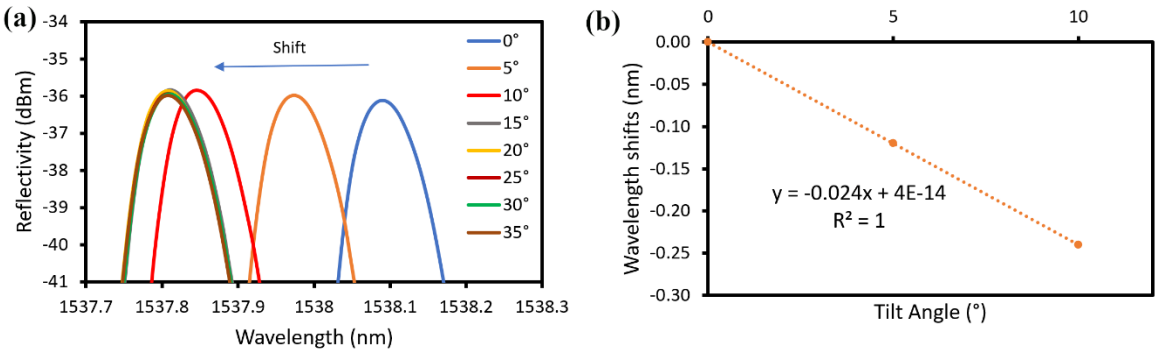

Figure 9(a) A closer view of FBG 2 blueshift during 0° to 40° tilt and (b) The linear response of FBG 2 in terms of wavelength shifts during 0° to 40° tilt.

However, when the sensor is tilted towards the +x direction, only FBG 1 is significant. At the same time, the compressional reading of FBG 2 only verifies that the sensor is tilted toward the +x direction and not towards -x. A similar concept can be applied when the tilt sensor is tilted towards the -x direction, where only the reading of FBG 2 is significant for the tilt angle measurement.

4.2. Field test

We obtained the sensor sensitivity of 0.0215 nm per degree of tilt from the laboratory calibration earlier. By referring to Equation 5 below, the current tilt angle of the inclinometer, θ, can be obtained by dividing the wavelength shift obtained during the measurement, $\Delta\lambda_B$ with the sensitivity value obtained during calibration of 0.0215 nm/°.

$$\frac{0.0215nm}{1°} = \frac{\Delta\lambda_B}{\theta} \quad (5)$$

Further, from trigonometry, the current displacement at a certain depth, *x*, can be obtained by multiplying $sin\ \theta$ with the length of the sensor, *l*.

Journal Pre-proof

$$sin\ \theta = \frac{x}{l} \tag{6}$$

The casing's inclination profiles captured by the inclinometer during the field test were constructed by plotting the casing's depth versus horizontal displacement. Both results are illustrated in Figure 10 and Figure 11.

Figure 10(a) illustrates the horizontal displacement of the inclinometer casing captured by S1 when the casing was pulled 0.5 m and 1 m from the vertical axis. The inclinometer could follow the casing's shape, simulating a possible slope or ground movement. The reading from S1 matches the measurements of a conventional, 70 cm inclinometer probe currently widely used. Furthermore, in Figure 10(b), our proposed inclinometer shows a better measurement resolution within the same probe length, providing a more detailed mapping of the casing by combining all data points from S1, S2, and S3.

Journal Pre-proof

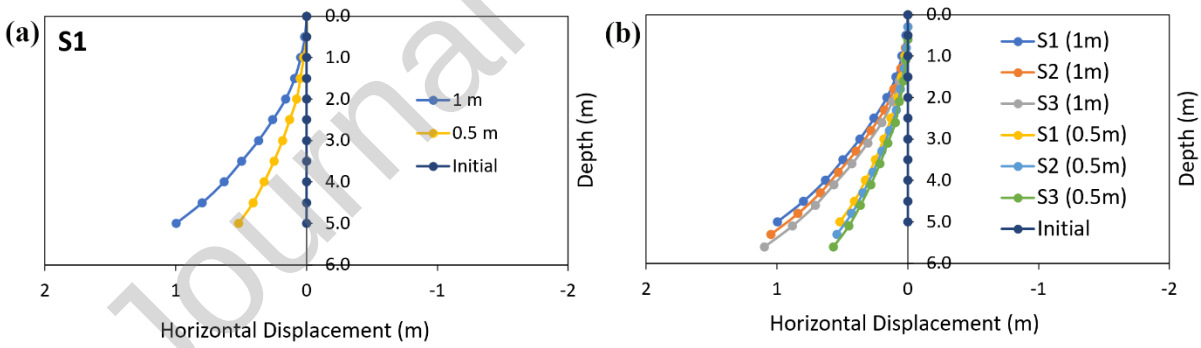

Figure 10. The horizontal displacement of the inclinometer casing was measured by (a) S1 and (b) all the sensors when the bottom of the casing was pulled 0.5 m and 1 m.

Figure 11(a) illustrates the horizontal displacement of the casing captured by the sensor S1 during Test 2. This plot further verifies the results in Figure 10, in which the device successfully maps the horizontal displacement of the casing along with a depth of 5 m. A more detailed illustration of the casing's displacement is given in Figure 11(b) when all the readings from S1, S2, and S3 are combined. Compared to Figure 11(a), the presence of three sensors provides a better measurement resolution of the casing's displacement profile than only one

sensor in the widely used conventional inclinometer nowadays. Although the traditional inclinometer probe could be inserted into the casing in a smaller depth interval to obtain the same resolution, this could cost the user a lot of time to complete a single measurement. Therefore, it is proven that the proposed FBG-based inclinometer could provide more data than the conventional inclinometer probe within 10 measurements taken (0.5 m to 5.0 m depth).

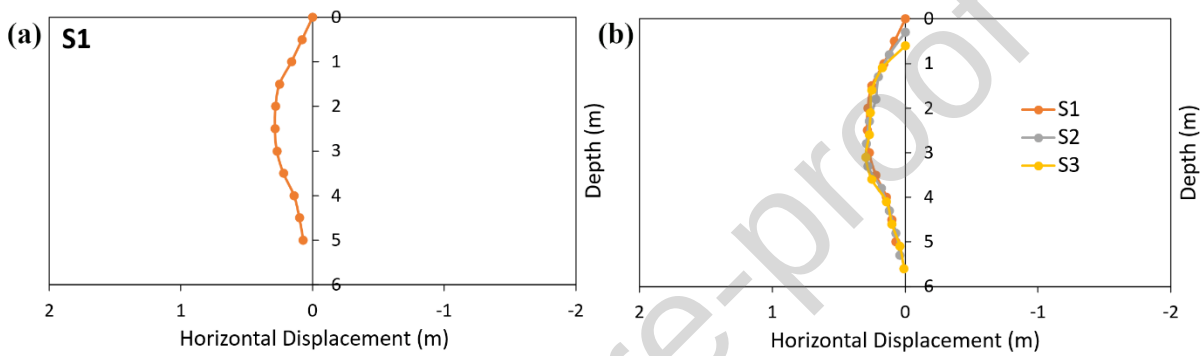

Figure 11. The horizontal displacement of the inclinometer casing as measured by (a) S1 and (b) all the sensors when the middle part of the casing was pulled 0.3 m.

In addition, a table of comparison is given in Table 1 between our proposed inclinometer and the previous works. Compared to previous work, the most significant feature of our inclinometer is the compact design of the tilt sensor with an enhanced sensitivity value.

Table 1. Table of comparison between the proposed inclinometer with previous designs

Type	No. of sensors	Material	Sensors Dimensions L x W	Resolution/ sensitivity (nm/°)	Range (+/-)	Reference
Conventional MEMS	1	Metal	68cm x 2.5cm	0.001°	30°	[28]
Optical-based sensor	1	Titanium	16cm x 5cm	0.06 nm/°	15°	[11]

Journal Pre-proof

Optical-based sensor	1	Silica	-	0.014 nm/°	14°	[10]
Optical-based sensor	1	PLA	12cm x 7.5cm	0.01 nm/°	90°	[21]
Optical-based sensor	1	PLA	6.2cm x 1.2cm	0.01 nm/°	90	[20]
Optical-based sensor	3	TPU	7cm x 2cm	0.0215 nm/°	40°	This work

Previous sensors reported above have only utilized only one sensor in the inclinometer. The compact feature of the tilt sensors in this work enables us to install three sensors within a 70 cm-length inclinometer, enhancing the resolution of the measured slope profile. Three sensors also provide additional data regarding the casing displacement at a certain depth compared to the conventional inclinometer probe, which requires the user to carry out extra measurements with extra cost and time. Besides that, the sensitivity of this device is also higher than most of the previous designs by a factor of two, owing to the elasticity of the TPU as the middle shaft. Previous sensors with materials such as metal [28] and titanium [11] can be stiff and rigid, reducing the device's sensitivity. The table also shows that no reported design in the past fabricated its sensors using TPU as the middle shaft. Overall, the proposed inclinometer outperformed the designs by others in terms of the sensor's size and sensitivity value which highlights the importance of the proposed inclinometer in the advancements of optical-based sensors.

Conclusion

An FBG-based inclinometer probe was fabricated using a 3D printer comprising three highly compact tilt sensors with a TPU-based intermediate shaft. The laboratory tested and calibrated sensors with a sensitivity value of 0.0215 nm/°, which is relatively higher than the currently reported optical-based inclinometer. It was then further tested for real field applications where the inclinometer was inserted into a 6 m long inclinometer casing that attached vertically to a 3-story building.

Journal Pre-proof

The horizontal displacement plots of the casing show promising results regarding the functionality of the proposed inclinometer, which can map the horizontal displacement of the casing. The presence of three sensors enables the device to obtain more data at a certain depth, hence providing a better resolution of the inclination profile compared to the conventional inclinometer probe. Furthermore, it has also been proven that the strain-free FBG T was unaffected by the tilt measurement, providing the temperature compensation factor for the device. A highly sensitive, 3D printed, FBG-based inclinometer probe equipped with a temperature-compensated factor is a promising solution and alternative to the current conventional inclinometers in geotechnical applications.

Acknowledgments

The authors are pleased to acknowledge the support of the Universiti Malaya through grant number UM-Innovate PPSI-2020-HICOE-02 and from the British Council-MIGHT NUOF with grant number IF022-2020. Grattan also acknowledges the support from the Royal Academy of Engineering.

References

[1] P. Ferdinand, S. Magne, V. Dewynter-Marty, S. Rougeault, L. Maurin, Applications of Fiber Bragg Grating sensors in the composite industry, MRS Bull. 27 (2002) 400–407. https://doi.org/https://doi.org/10.1557/mrs2002.126.

[2] Slope Profiles Part 1: Calculating with Slope Angles – Elisha Anne Teo, PhD, (n.d.). https://elisharesearch.com/2015/01/23/calculating-with-angles/ (accessed December 26, 2022).

[3] Slope profile – Field Studies Council, (n.d.). https://www.field-studies-council.org/resources/16-18-biology/fieldwork-techniques/abiotic-factors/slope-profile/ (accessed December 26, 2022).

[4] G. Machan, V.G. Bennett, Use of inclinometers for geotechnical instrumentation on transportation projects: State of the practice, Transp. Res. Circ. E-C129 (2008) 92p. https://doi.org/10.17226/23074.

Journal Pre-proof

[5] Z. Mihalinec, M. Bačić, M.S. Kovačević, Risk identification in landslide monitoring, Gradjevinar. 65 (2013) 523–536. https://doi.org/10.14256/jce.717.2012.

[6] R. Olaru, C. Cotae, Tilt sensor with magnetic liquid, Sensors Actuators, A Phys. 59 (1997) 133–135. https://doi.org/10.1016/S0924-4247(97)80162-8.

[7] M. Drahansky, Liveness Detection in Biometrics, in: G. Chetty, J. Yang (Eds.), Adv. Biometric Technol., IntechOpen, Rijeka, (2011) 179-198. https://doi.org/10.5772/17205.

[8] MF Ghazali, H. Mohamad, K.A. Ang, Development of distributed fibre optic inclinometer for landslide and geotechnical application, in: 16th Asian Reg. Conf. Soil Mech. Geotech. Eng. ARC 2019, 2020: pp. 3–6.

[9] L. Schenato, L. Palmieri, M. Camporese, S. Bersan, S. Cola, A. Pasuto, A. Galtarossa, P. Salandin, P. Simonini, Distributed optical fibre sensing for early detection of shallow landslides triggering, Sci. Rep. 7 (2017) 1–7. https://doi.org/10.1038/s41598-017-12610-1.

[10] L.M.N. Amaral, O. Frazão, J.L. Santos, A.B. Lobo Ribeiro, Fiber-optic inclinometer based on taper Michelson interferometer, IEEE Sens. J. 11 (2011) 1811–1814. https://doi.org/10.1109/JSEN.2011.2105264.

[11] Y. Yang, X. Ma, K. Chen, E. Wang, Z. Yu, Q. Yu, A high-resolution dynamic fiber-optic inclinometer, Sensors Actuators, A Phys. 283 (2018) 305–312. https://doi.org/10.1016/j.sna.2018.10.007.

[12] M. Maheshwari, Y. Yang, D. Upadrashta, T. Chaturvedi, A Rotation Independent In-Place Inclinometer/Tilt Sensor Based on Fiber Bragg Grating, IEEE Trans. Instrum. Meas. 68 (2019) 2943–2953. https://doi.org/10.1109/TIM.2018.2870246.

[13] C. Hong, Y. Zhang, Z. Lu, Z. Yin, A FBG Tilt Sensor Fabricated Using 3D Printing Technique for Monitoring Ground Movement, IEEE Sens. J. 19 (2019) 6392–6399. https://doi.org/10.1109/JSEN.2019.2908873.

[14] S. He, X. Dong, K. Ni, Y. Jin, C.C. Chan, P. Shum, Temperature-insensitive 2D tilt sensor with three fiber bragg gratings, Meas. Sci. Technol. 21 (2010) 025203.

Journal Pre-proof

https://doi.org/10.1088/0957-0233/21/2/025203.

[15] H.Y. Au, S.K. Khijwania, H.Y. Fu, W.H. Chung, H.Y. Tam, Temperature-insensitive fiber bragg grating based Tilt sensor with large dynamic range, J. Light. Technol. 29 (2011) 1714–1720. https://doi.org/10.1109/JLT.2011.2132695.

[16] H. Bao, X. Dong, L.Y. Shao, C.L. Zhao, S. Jin, Temperature-insensitive 2-D tilt sensor by incorporating fiber Bragg gratings with a hybrid pendulum, Opt. Commun. 283 (2010) 5021–5024. https://doi.org/10.1016/j.optcom.2010.07.050.

[17] X. Dong, L. Hu, L. Shao, Y. Wang, J. Zheng, Temperature-insensitive 2D fiber Bragg grating TILT sensor, Microw. Opt. Technol. Lett. 55 (2013) 344–346. https://doi.org/10.1002/mop.27281.

[18] Y.L. Wang, B. Shi, T.L. Zhang, H.H. Zhu, Q. Jie, Q. Sun, Introduction to an FBG-based inclinometer and its application to landslide monitoring, J. Civ. Struct. Heal. Monit. 5 (2015) 645–653. https://doi.org/10.1007/s13349-015-0129-4.

[19] K. Ni, X. Dong, Y. Jin, H. Xu, Temperature-independent fiber Bragg grating tilt sensor, Microw. Opt. Technol. Lett. 52 (2010) 2250–2252. https://doi.org/10.1002/mop.25425.

[20] N.N. Ismail, M.S.M. Sa'ad, M.F. Ismail, M.K.A. Zaini, K.S. Lim, K.T.V. Grattan, G. Brambilla, B.M.A. Rahman, H. Mohamad, H. Ahmad, Biaxial 3D-Printed Inclinometer Based on Fiber Bragg Grating Technology, IEEE Sens. J. 21 (2021) 18815–18822. https://doi.org/10.1109/JSEN.2021.3090105.

[21] N.N. Ismail, A.S. Sharbirin, M.S.M. Sa'ad, M.K.A. Zaini, M.F. Ismail, G. Brambilla, B.M.A. Rahman, K.T.V. Grattan, H. Ahmad, Novel 3D-printed biaxial tilt sensor based on fiber Bragg grating sensing approach, Sensors Actuators, A Phys. 330 (2021) 112864. https://doi.org/10.1016/j.sna.2021.112864.

[22] A.D. Kersey, M.A. Davis, H.J. Patrick, M. LeBlanc, K.P. Koo, C.G. Askins, M.A. Putnam, E.J. Friebele, Fiber grating sensors, J. Light. Technol. 15 (1997) 1442–1462. https://doi.org/10.1109/50.618377.

[23] H. Bao, X. Dong, H. Gong, C.C. Chan, P. Shum, Temperature-insensitive FBG tilt sensor

Journal Pre-proof

with a large measurement range, in: 2009 Asia Commun. Photonics Conf. Exhib., IEEE, 2009: pp. 1–5. https://doi.org/https://doi.org/10.1016/j.optcom.2009.11.014.

[24] Urethane thermoplastic elastomer (TPU) - Thermoplastic Polyurethane (TPU) - Matmatch, (n.d.). https://matmatch.com/materials/mbas116-urethane-thermoplastic-elastomer-tpu- (accessed December 26, 2022).

[25] H. Lee, R.I. Eom, Y. Lee, Evaluation of the mechanical properties of porous thermoplastic polyurethane obtained by 3D printing for protective gear, Adv. Mater. Sci. Eng. 2019 (2019) 5838361. https://doi.org/10.1155/2019/5838361.

[26] C. Hong, Y. Zhang, L. Borana, Design, fabrication and testing of a 3D printed FBG pressure sensor, IEEE Access. 7 (2019) 38577–38583. https://doi.org/10.1109/ACCESS.2019.2905349.

[27] V.C. Pinto, T. Ramos, S. Alves, J. Xavier, P. Tavares, PMGP Moreira, R.M. Guedes, Comparative Failure Analysis of PLA, PLA/GNP and PLA/CNT-COOH Biodegradable Nanocomposites thin Films, Procedia Eng. 114 (2015) 635–642. https://doi.org/10.1016/j.proeng.2015.08.004.

[28] [Updated] Inclinometers: Types, How They Work, & Functions, (n.d.). https://www.encardio.com/blog/inclinometer-types-how-it-works-uses/ (accessed July 4, 2022).

Journal Pre-proof

Biographies

Muhammad Syamil Mohd Sa'ad received the Bachelor of Science (Hons) in Pure Physics from the Faculty of Science, University of Malaya. He is currently a postgraduate student and a research assistant at the Photonics Research Center, University of Malaya. His research interest focuses on fiber optic sensors mainly on fiber Bragg gratings.

Harith Ahmad received a Ph.D. in laser technology from the University of Wales, Swansea, U.K. in 1983. He is currently a Professor with the Department of Physics and director of the Photonics Research Center, Universiti Malaya where he had actively pursued research activities in the field of photonics since 1983. He has authored more than 400 professional papers in international journals and conferences. His research interests are in lasers, fiber-based devices for telecommunications, and fiber-based sensor devices.

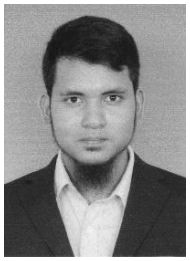

Muhamad Zharif Samion obtained his Bachelor of Engineering (Electrical) from the Faculty of Engineering, University of Malaya in 2015 and his Doctor of Philosophy (PhD) in Photonics Engineering at the Photonics Research Centre, University of Malaya in 2021. His research focuses on pulsed and multiwavelength fibre lasers.

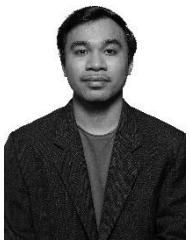

Mohamad Ashraff Alias received the Bachelor of Science (Hons) in Industrial Physics from the Faculty of Science, Universiti Teknologi Malaysia (UTM) in 2020. He is currently a postgraduate student and a research assistant at the Photonics Research Centre, University of Malaya. His current research interest focuses on optical fiber sensors mainly on fiber Bragg gratings.

Muhammad Khairol Annuar Zaini received a bachelor's degree from the Department of Physics, Faculty of Science, University Putra Malaysia, Malaysia, in 2015, followed by a Ph.D. from University of Malaya. His current research interest includes fiber Bragg grating sensors and Spatial Division Multiplexing.

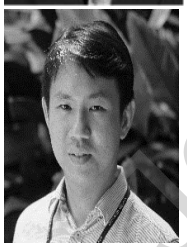

Lim Kok Sing received the B.E. degree from the Department of Electrical Engineering, Faculty of Engineering, Universiti Malaya, Malaysia, in 2008, and the Ph.D. degree from the Photonics Research Centre, Universiti Malaya, in 2012. He is currently a Senior Lecturer with the Photonics Research Centre, University of Malaya. He is a Corporate Member of the Institute of Engineers Malaysia (IEM), a registered Professional Engineer (Telecommunication) of the Board of Engineers Malaysia (BEM), and a member of OSA.

Kenneth T.V. Grattan graduated in Physics from Queen's University Belfast with a BSc (First Class Honours) in 1974, followed by a Ph.D. in Laser Physics. He obtained the degree of Doctor of Science (DSc) from City University in 1992 for his sensor work. His research interests have expanded to include the development and use of fiber optic and optical systems in the measurement of a range of physical and chemical parameters.

Journal Pre-proof

B.M. Azizur Rahman received BSc Eng and MSc Eng degrees in Electrical Engineering with distinctions from Bangladesh University of Engineering and Technology (BUET), Dhaka, Bangladesh, in 1976 and 1979, respectively He received his Ph.D. degree in Electronic Engineering from University College, London in 1982. At City University, he leads the research group on Photonics Modelling.

Gilberto Brambilla is a professor at the Optoelectronics Research Centre and, co-Director and General Manager of the Future Photonics Hub. He obtained his MSc (Engineering) with honors from Politecnico di Milano (Italy) in 1996 and his Ph.D. degree in Optoelectronics from the University of Southampton in 2002. His research interests include optical fiber sensors; optical fiber structuring using fs lasers; specialty and polymer fibers; new fiber fabrication technologies and fibers for nuclear sensing.

Sulaiman Wadi Harun received his bachelor's degree in Electrical and Electronics System Engineering from Nagaoka University of Technology, Japan, in 1996, and his master's and doctoral degrees in Photonics Technology from the University of Malaya in 2001 and 2004, respectively. He has more than 20 years of research experience in the development of optical fiber devices including fiber amplifiers, fiber lasers, and fiber optic sensors. Professor Harun has published more than 900 articles in reputable ISI journals, and his papers have been cited more than 8000 times with an h-index of more than 40, showing the impact on the community. He is the Fellow of the Malaysian Academic of Science, and the founder and honorary advisor for the Optical Society of Malaysia.

Mohammad Faizal Ismail obtained his Bachelor of Engineering (Telecommunication) from the Faculty of Engineering, University of Malaya in 1999 and Master of Engineering (Science) from the Faculty of Engineering, University of Malaya in 2004. He obtained a Ph.D. from the same university in 2021 where his research focuses on pulsed, multiwavelength fiber lasers and waveguides.

Journal Pre-Proof

CRediT Authorship Contribution Statement

Muhammad Syamil Mohd Sa'ad: Conceptualization, Investigation, Methodology, Formal Analysis, Visualization, Writing – Original Draft**. Harith Ahmad**: Conceptualization, Validation, Writing – Review & Editing**. Muhamad Zharif Samion**: Conceptualization, Validation, Writing – Review & Editing**. Mohamad Ashraff Alias**: Investigation, Methodology, Writing – Original Draft**. Muhammad Khairol Annuar Zaini**: Resources, Writing – Original Draft**. Lim Kok Sing**: Resources, Writing – Original Draft**. Kenneth T. V. Grattan**: Writing – Review & Editing**. B. M. Azizur Rahman**: Writing – Review & Editing**. Gilberto Brambilla**: Writing – Review & Editing**. Sulaiman Wadi Harun**: Resources, Formal Analysis, Visualization**. Mohammad Faizal Ismail**: Resources, Conceptualization, Methodology, Writing – Original Draft

Declaration of Competing Interest

The authors declare that they have no known competing financial interests or personal relationships that could have appeared to influence the work reported in this paper.

Graphical abstract

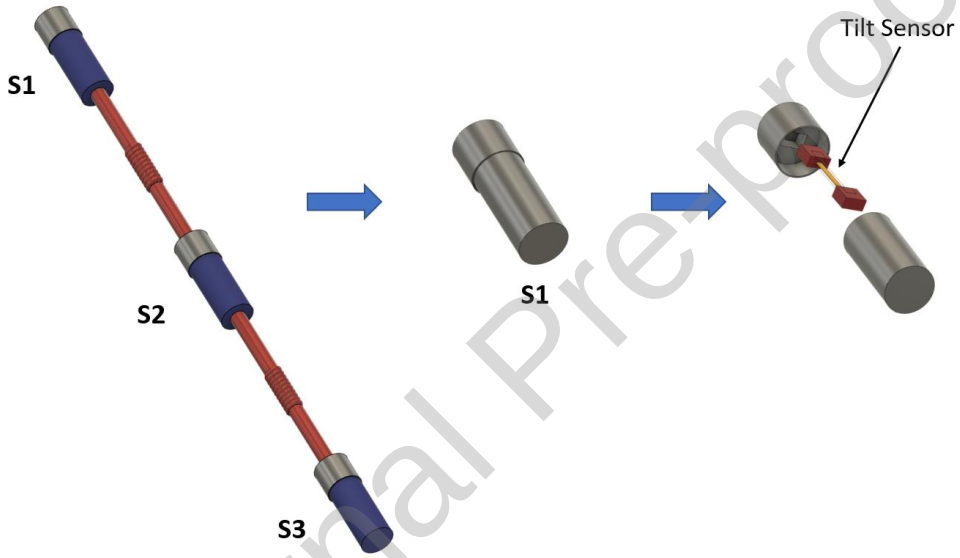

Journal Pre-proof

HIGHLIGHTS

- The inclinometer probe was equipped with 3 highly compact tilt sensors.
- The tilt sensors possess an elastic middle shaft that was 3D-printed using the Thermoplastic Polyurethane (TPU).
- The probe yields a higher sensitivity value which leads to the improvement in the tilt angle resolution.
- The device also provides a higher resolution of the inclination profile measurements.
- FBGs were used due to its immunity against electromagnetic interference and short circuits.
- An extra Fiber Bragg Grating is added to this design as a temperature sensor to compensate the shift due to the change in temperature.